APPLICATION OF THE KIHARA CORE MODEL EQUATION

TO GAS-SOLID INTERACTIONS

A THESIS

Presented to

The Faculty of the Division of Graduate

Studies and Research
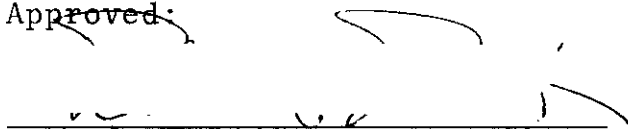
By

Malton Joseph Bullock, Jr.

In Partial Fulfillment

of the Requirements for the Degree

Master of Science in Chemistry

Georgia Institute of Technology

March, 1974

APPLICATION OF THE KIHARA CORE MODEL EQUATION

TO GAS-SOLID INTERACTIONS

Approved:

Robert A. Pierotti, Chairman

George A. Miller

Peter E. Sturrock

Date approved by Chairman: 1 May 1974

ACKNOWLEDGMENTS

TABLE OF CONTENTS

LIST OF TABLES

LIST OF ILLUSTRATIONS

LIST OF SYMBOLS AND ABBREVIATIONS

a   constant proportional to the adhesion between molecules

A   1. area
          2. the first gas virial coefficient

b   1. constant proportional to the volume of the molecule
          2. constant equal to $\frac{1}{P(\theta=1/2)}$

$b_0(r)$ the second virial coefficient for a rigid sphere of diameter r

B   the second gas virial coefficient

B_{is} the ith gas-solid virial coefficient

B_{2s} the second gas-solid virial coefficient

c   constant

C   1. the third gas virial coefficient
          2. the core of a parallel body

f   1. a factor which indicates deviation from rigid sphere behavior
          2. the fugacity of the adsorbate in the bulk gas phase

k   the Boltzmann constant

K   constant

l_i length of the ith edge of a molecule

m   the index of attraction in the Lennard-Jones (m-n) potential

M   surface integral of the mean curvature of a parallel body

M_0 surface integral of the mean curvature of the core of a molecule

n   1. the number of moles
          2. the index of repulsion in the Lennard-Jones (m-n) potential

n_t total number of moles of gas in the sample cell volume

N the number of molecules in the gas

N_a the number of moles of gas adsorbed

N_o Avogadro's number

p pressure

P_o the saturated vapor pressure of liquid adsorbate at the isotherm temperature

r
1. radius of a spherical molecule
2. diameter of a rigid sphere
3. intermolecular distance

R Boltzmann's constant multiplied by Avogadro's number

S surface area of a parallel body

S_o surface area of the core of a molecule

T absolute temperature

U interaction energy between a gas adsorbate and the adsorbent

U_o value of the potential minimum for the core model of molecular interactions

U_{OAB} value of the potential minimum for the core model of molecules A and B

V_a volume of gas adsorbed

V_m
1. volume of a single molecule
2. volume of gas in a monolayer

V
1. volume
2. volume of a parallel body

V_{app} apparent volume

V_{ex} excess volume

V_{geo} geometric volume

V_o volume of the core of a molecule

$\bar{V}$ molar volume

z vertical distance from the center of an adsorbate molecule to the adsorbing surface

z_o vertical distance from the center of an adsorbate molecule to the adsorbent surface when the interaction energy is zero

z^* vertical distance from the center of an adsorbate molecule to the adsorbent surface at the potential minimum ε^*

Greek Symbols:

α_i angle made by the ith edge

$\Gamma()$ the gamma function

ε potential of molecular interaction

ε^* depth of the single gas molecule-solid potential well

ε^*_{30} depth of the molecular pair potential well

θ fraction of surface sites covered by adsorbate

π two-dimensional spreading pressure

ρ the shortest distance between molecular cores

ρ_o the shortest distance between cores at the potential minimum U_o

ρ_{OAA} the shortest distance between cores of two like molecules of gas A at the potential minimum

ρ_{OAB} the shortest distance between cores of unlike molecules A and B at the potential minimum

ρ_{OBB} the shortest distance between cores of two like molecules of gas B at the potential minimum

SUMMARY

A preliminary investigation is presented concerning
the possible application of the Kihara core model theory
used in the study of non-spherical gas molecules to physical
adsorption studies. The theory is based on Kihara's defi-
nition of the core of the molecule which has physical
dimensions greater than the point center used with many gas
studies but at the same time is confined within the molecular
limits.

The three adsorbate-adsorbent systems investigated
are the benzene-graphite system, the carbon dioxide-graphite
system, and the argon-graphite system. Core values are
calculated for the adsorbent graphite and one of the adsor-
bates, argon. Core values for benzene and carbon dioxide are
taken from Kihara's calculations.

The core values are used in the Kihara equation to
calculate the Kihara parameters $\frac{U_o}{k}$ and ρ_o which best fit
experimental data. $\frac{U_o}{k}$ is set equal to $\frac{\varepsilon^*}{k}$ for the system under
investigation, and ρ_o is adjusted until the second gas-solid
virial coefficient corresponding to a given temperature is
correctly calculated by use of the Kihara equation. The
value of ρ_o calculated for the benzene-graphite system is
smaller than expected. The values of ρ_o calculated for the
carbon dioxide-graphite system and argon-graphite system are
larger than expected.

CHAPTER I

INTRODUCTION

The study of gases and their interactions with one
another has been taking place for many years by physical
chemists. By using existing laws of chemistry and physics,
new theories are developed based upon experimental work.
These theories are usually expressed in the form of a mathe-
matical model. This model is tested on other systems and if
necessary modified with more complete experimental information
so that the behavior of unstudied systems can be predicted
without making measurements. A model may become widely
accepted even though it does not describe a system accurately
or is only useful over short ranges. In these cases empirical
equations are generally formulated which give good agreement
with experimental findings but yield no information on funda-
mental molecular interactions.

Ideal Gases

The ideal gas equation came about as the result of
work done mainly by three men. In 1662, Robert Boyle deter-
mined that the volume of a given amount of gas at constant
temperature was inversely proportional to the pressure,
stated mathematically as

$$V = constant/P \qquad (1)$$

where

P = the pressure exerted by a gas in volume V

V = the volume of the gas.

In 1802, Gay-Lussac reported that the volume of a given amount of gas at constant pressure was directly proportional to the absolute temperature. This can be written as

$$V = constant \times T \qquad (2)$$

where

T = the absolute temperature.

Avogodro's law, stating that equal volumes of gases at the same temperature and pressure contain the same number of molecules, was combined with relationships (1) and (2) to give the ideal gas equation

$$\frac{PV}{nT} = constant \qquad (3)$$

where

n = the number of moles of gas.

The ideal gas equation did not apply very well to most real systems; therefore, new and better relationships were called

for.

Real Gases

In 1879, Van der Waals reported a variation of the ideal gas equation[2]

$$(P + \frac{n^2 a}{V^2})(V - nb) = hRT \tag{4}$$

where

a = a constant proportional to the cohesion between molecules

b = a constant proportional to the volume of the molecules.

The $\frac{n^2 a}{V^2}$ term represents the attractive force between real molecules that does not exist in the ideal state. The nb term is called the excluded volume of n moles of the gas.

Further attempts to explain the gas phase over the entire temperature-pressure range saw the development of more empirical relationships, some of which, for example those of Clausius[1] and Berthelot[3], were modifications of Van der Waals' equation. Dieterici[3] developed an equation with an exponential factor. Beattie and Bridgeman[3] introduced a five parameter equation, and Benedict, Webb, and Rubin[3] used an eight parameter equation in order to fit certain experimental data.

In 1901, Kamerlingh Onnes[3] fit compressibility data to what is now called the virial equation of state for real

gases. For a given temperature this equation relates the compressibility factor to a Taylor series in the power of 1/V as

$$\frac{P\overline{V}}{RT} = A + \frac{B}{\overline{V}} + \frac{C}{\overline{V}^2} + \dots \tag{5}$$

where

A = the first gas virial coefficient

B = the second gas virial coefficient

C = the third gas virial coefficient

R = the gas constant

$\overline{V}$ = the molar volume.

By means of statistical mechanics the virial coefficients may be expressed in terms of intermolecular potential functions. It is therefore possible to obtain a quantitative interpretation of the deviations from the ideal gas law in terms of the forces between molecules.

For spherically symmetrical molecules the second gas virial coefficient can be written in integral form as[3]

$$B = 2\pi N_o \int_0^\infty (1 - e^{-\frac{U(\infty)}{kT}}) r^2 dr \tag{6}$$

where

r = the intermolecular distance

U(∞) = the potential of molecular interaction

N_o = Avogadro's number

k = the Boltzmann constant.

The exact nature of the intermolecular potential is not known but generally a Lennard-Jones 6-12 form can be used when the gas is monatomic or consists of spherically symmetric molecules. The potential, $\varepsilon(r)$, can then be expressed in terms of the two parameters ε_{3D}^* and r_o, where r_o is the distance between molecular centers when the interaction energy is zero and r_e is the separation at the potential minimum, ε_{3D}^* (Figure 1).

Several theories have been developed in attempts to calculate the second virial coefficients for non-spherical molecules. Isihara[3] took an earlier treatment which showed the second virial coefficient for rigid spheres to be equal to four times the volume of the molecules in the gas and extended it to rigid non-spherical molecules. The resultant equation was

$$B = 4 N v_m f \tag{7}$$

where

N = the number of molecules in the gas

v_m = the volume of a single molecule

f = a factor which indicates deviation from rigid sphere behavior.

For each molecule tested the factor f was calculated by the
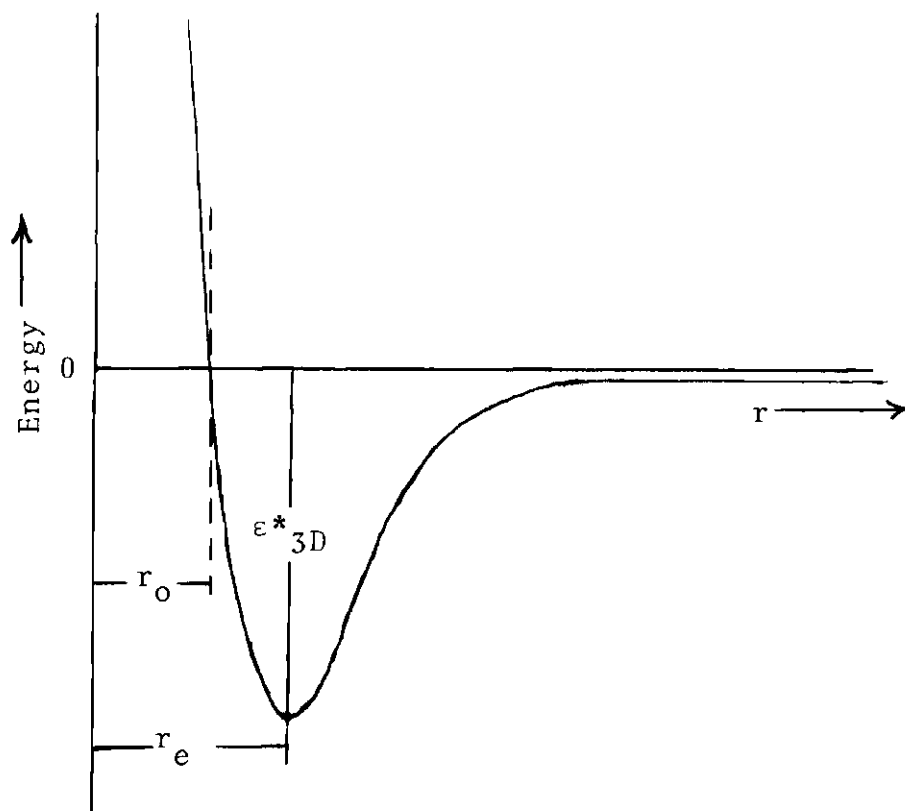
Figure 1.   Lennard Jones (6-12) Potential for Two
            Molecules

use of group theory and differential geometry.

In 1948, Corner[3] developed a theory to study the second virial coefficients for long molecules. He adopted a four-center model in which the molecule is represented by four centers of force distributed along a line dependent on the molecular length. Kihara took the results from Isihara's treatment and extended them to obtain expressions for the second virial coefficient of angle dependent Lennard-Jones molecules[3]. An extension of Kihara's core model theory to unlike, non-spherical molecules is presented in Chapter II.

Adsorption

Adsorption is the production of a concentration gradient near the surface of a solid placed in a gaseous atmosphere. The magnitude of the adsorption is dependent on temperature, gas pressure, surface structure, interactions between gas molecules and atoms of the solid, and the lateral interactions between adsorbed molecules. Adsorption can be divided into chemical adsorption (chemisorption) and physical adsorption (physisorption). Chemisorption occurs with electron transfer or orbital overlap and the production of heat usually much higher than the heat of vaporization of the adsorbate. Physisorption will occur with any gas-solid system. It is an exothermic process with the heat produced being of the same order of magnitude as the adsorbate heat of vaporization.

It is convenient to conduct physisorption studies with an adsorbate near its normal boiling point. In this region condensation simulates adsorption. As the pressure is increased, condensation continues until a monolayer is formed. Further increases in gas pressure will then produce multi-layers. In physical adsorption measurements, the amount of gas adsorbed is calculated by introducing a known amount of gas into a known volume at a given temperature, calculating the amount of gas present from pressure readings, and subtracting the calculated amount from the initial amount. An isotherm is made by taking a series of measurements at a constant temperature by varying the pressure, and a plot of gas adsorbed versus pressure is made for each temperature. A series of isotherms taken on one adsorbate-adsorbent system is used to extract thermodynamic data concerning that system.

Three major approaches have been used in attempts to explain physical adsorption. The first of these methods treats adsorbed molecules as being localized at a particular site on the adsorbent surface, while the remaining two methods treat the adsorbed molecules as a two-dimensional phase along the plane of the adsorbent. The two-dimensional parameters, spreading pressure and area, can be more easily understood by assuming that a gas adsorbed on a solid will obey the same type two-dimensional equation found with low concentrations of fatty acids on water. The behavior of these films at low concentrations is approximated by the two-dimensional ideal

gas law

$$\pi A = RT \tag{8}$$

where

π = the spreading pressure

A = the average area available to a mole of molecules in the surface film

R = Boltzmann's constant multiplied by Avogodro's number

T = the absolute temperature

By the use of the Gibb's absorption equation, the equation

$$P = K\theta \tag{9}$$

where

K = a constant

θ = a fractional surface coverage

can be derived which is the adsorption equivalent of the Henry's law equation when dealing with dilute solutions. It is generally applicable in the linear low coverage portion of an isotherm referred to as the Henry's law region, and K is known as the Henry's law constant.

In 1918, Langmuir developed what is known as the Langmuir isotherm equation

$$\theta = \frac{bP}{1+bP} \tag{10}$$

where

b = a constant equal to $\dfrac{1}{P_{(\theta=1/2)}}$

θ = the fraction of surface sites covered by adsorbate

using the localized model and assuming negligible interactions between neighboring sites and adsorbate. It is evident that at high pressures the maximum coverage predicted will be that of a monolayer, which therefore limits its use to the submonolayer region. In the low pressure region Henry's law behavior is predicted as the term bP becomes negligible in comparison with one in the denominator[1].

In 1938, Brunauer, Emmett, and Teller[2] developed an adsorption isotherm equation, assuming localized sites, which provided for multilayer formation. The BET equation can be written

$$\frac{P}{V_A(P_o-P)} = \frac{1}{V_m C} + \frac{(C-1)P}{V_m\, C\, P_o} \tag{11}$$

where

C = a constant

V_A = the volume of gas adsorbed

V_m = the volume of gas in a monolayer

P = the pressure

P_o = the saturated vapor pressure of liquid adsorbate

at the isotherm temperature.

Other assumptions made were that all surface sites are equivalent, stacking takes place on previously adsorbed molecules at localized sites, lateral interactions between adsorbed molecules are negligible, and the heat of vaporization of layers above the initial monolayer is equivalent to the heat of vaporization of the bulk liquid. The BET equation has since been modified in attempts to account for lateral interactions.

Further attempts to account for lateral interactions included the development of mobile adsorption models from the two-dimensional form of gas equation of state and modification of existing liquid theories. One of the more recent liquid theory derivatives is that of Pierotti and McAlpin[4,5].

Virial Treatment of Adsorption

Many authors have applied the virial treatment of imperfect gases to adsorption by the use of statistical mechanics[6]. The equation produced expresses the amount of gas adsorbed by a solid as

$$N_a = \sum_{i \geq 1}^{\infty} B_{i+1,s} \, (f/RT)^i \tag{12}$$

where

B_{is} = the ith gas-solid virial coefficient

f = the fugacity of the adsorbate in the bulk gas phase

N_a = the number of moles of gas adsorbed.

The virial coefficients, B_{is}, are functions of temperature and are related to the interaction between individual gas molecules and the adsorbent surface and the interaction between adsorbed molecules. It is therefore possible to gain information about the adsorptive process by relating the virial coefficients to interaction parameters.

Halsey and co-workers were the first to relate virial coefficients to experimental adsorption and introduced the concept of apparent volume and excess volume[15]. Isotherm measurements were made in the Henry's law region where the only effective interaction is between individual gas molecules and the surface. Applying a Maxwell distribution to the gas phase, the apparent volume was given by the equation

$$V_{app} = \int_{V_{geo}} e^{-\frac{U}{kT}} \, dV \tag{13}$$

where

V_{app} = the apparent volume of the sample cell

V = the volume

V_{geo} = the geometric volume of the sample cell

U = the interaction energy between a gas molecule and the adsorbent.

(The apparent volume can also be given by the equation

$$V_{app} = n_t \frac{RT}{P} \tag{14}$$

where

n_t = the total number of moles of gas in the sample cell volume.)

The excess volume was given by the equation

$$V_{ex} = \int_{V_{geo}} (e^{-\frac{U}{kT}} - 1) dV \qquad (15)$$

where

V_{ex} = the excess volume.

A Sutherland type potential was used to describe the interaction between an adsorbate atom and adsorbent atom. It was also assumed that

$$U = 0 \qquad z \leqq z_o \qquad (16)$$

$$U = \frac{-\varepsilon^* z_o^3}{z^3} \qquad z > z_o \qquad (17)$$

where

ε^* = the potential minimum for interaction between an adsorbate molecule and the adsorbent

z = the vertical distance from the surface

z_o = the distance of closest approach.

After substituting this potential into the equation for excess volume and integrating, the result was

$$V_{ex} = Az_0 \sum_{j=0}^{\infty} (j!(3j-1))^{-1} (\frac{\varepsilon^*}{kT})^j \tag{18}$$

V_{ex} was determined experimentally, and Az_0 and $\frac{\varepsilon^*}{k}$ were adjusted until a best fit of the experimental data was obtained. The resulting ε^* was used with a Kirkwood-Muller equation to evaluate z_0. This approach allowed A to be calculated from Az_0.

The work of Halsey and co-workers up to this time had been done on poorly characterized surfaces. Shaeffer, Smith, and Polley developed a new homogeneous graphitized carbon black P33(2700) for use in physical adsorption studies, and Halsey and co-workers used it with many inert gas systems.

Sams, Constabaris, and Halsey[15] conducted extensive experimental work on P33 with the inert gases, methane, deuteromethane, hydrogen, and deuterium using the apparatus described by Constabaris, and the apparent cell volume was determined at several different pressures for each isotherm. The plot of apparent volume versus pressure was extrapolated to zero pressure and the apparent volume at zero pressure was determined. This apparent volume was equal to the sum of the geometric volume of the sample cell plus the second gas-solid virial coefficient, B_{2s}, defined as

$$B_{2s} = \int_{V_{geo}} (e^{-\frac{U}{kT}} - 1) dV. \tag{19}$$

Four potentials were used to analyze the data; (1) the Sutherland potential integrated over a semi-infinite solid, (2) a Lennard-Jones 6-12 potential integrated over a semi-infinite solid to yield a 3-9 potential, (3) a Lennard-Jones 6-12 potential integrated over a semi-infinite solid for the attractive part to yield a 3-12 potential, and (4) a Lennard-Jones 6-12 potential integrated over an infinite plane to yield a 4-10 potential. The Sutherland model was mentioned earlier. The Lennard-Jones models can be expressed in terms of the potential minimum ε^* and a position z_0 where the interaction energy is zero. These parameters are demonstrated in Figure 2 along with the variation of potential energy of an admolecule with its distance from the adsorbent surface.

The equation for B_{2s} has been solved analytically using the Lennard-Jones potential functions and integrating overall space (reasonable due to the short range interaction forces) to yield the equation

$$B_{2s} = Az_0 \; f(\frac{\varepsilon^*}{kT}) \qquad (20)$$

A locus of values was obtained for Az_0 and $f(\frac{\varepsilon^*}{kT})$ for each B_{2s} and a plot of Az_0 versus $f(\frac{\varepsilon^*}{kT})$ was made. When corresponding curves were drawn through the points for each B_{2s}, they intersected at a point which represented the best fit value of $\frac{\varepsilon^*}{k}$ and Az_0. The Sutherland model produced a poor
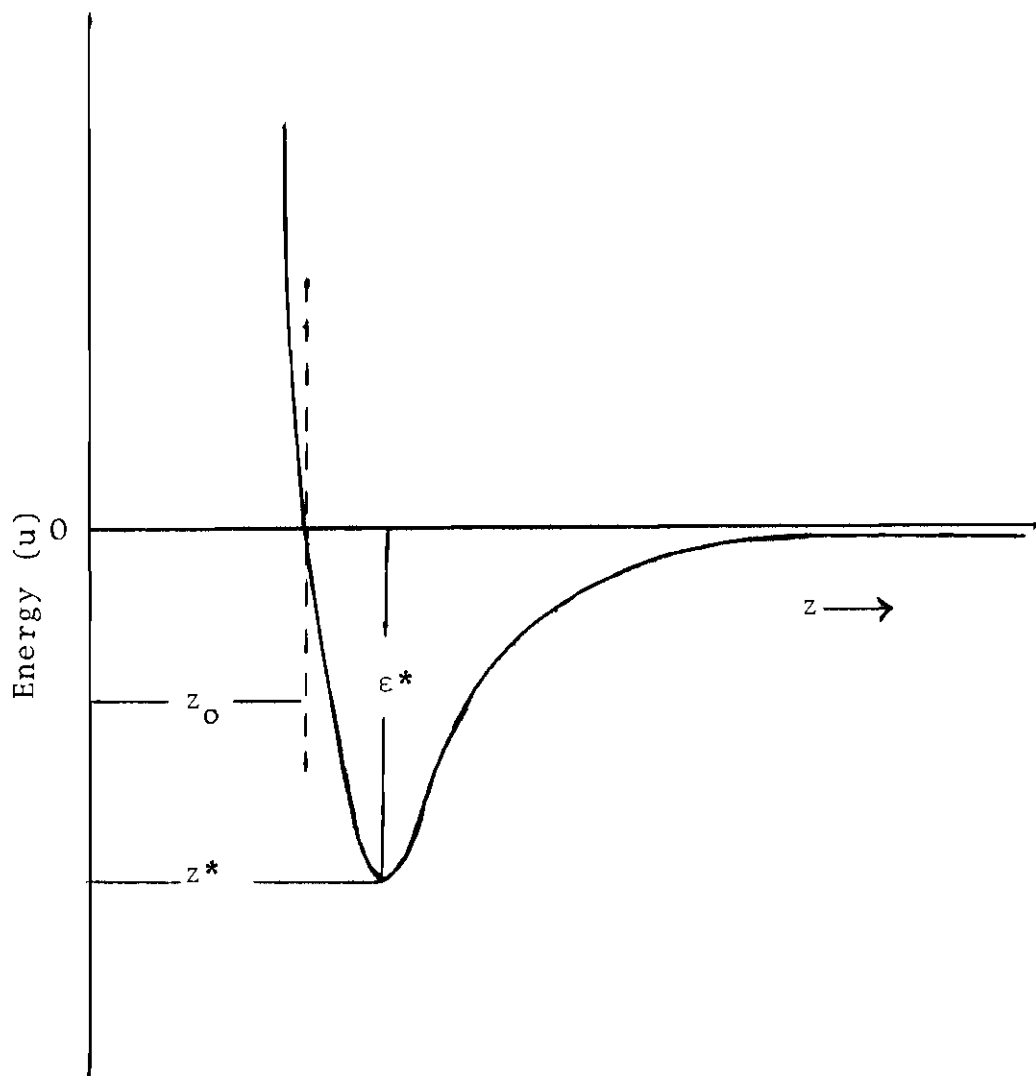
Figure 2. Potential Energy of an Adsorbate Molecule
as a Function of Distance from the
Adsorbent Surface. The Lennard-Jones
Parameters ε^* and z_o are Indicated.

fit, while the three models derived from the Lennard-Jones
6-12 potential were all reasonable and a best model was not
evident[7].

There have been other methods derived in attempts to
calculate various parameters necessary for a better under-
standing of gas-solid interactions, both spherical and non-
spherical[3,7]. Some of the methods are relatively simple but
are of value over a limited range of conditions. Such is the
case with the spherical potential. It gives reasonable
values for the parameters $\frac{\varepsilon^*}{k}$ and area if the adsorbate is
spherical, but when the adsorbate is non-spherical the area
is frequently too small by a factor of 100 or more while at
the same time a reasonable value of $\frac{\varepsilon^*}{k}$ is indicated. Some
of the methods give generally acceptable values for their
parameters but are of such complexity that they are difficult
to work with. An example is the use of a potential function
which accounts for hindered rotation to solve the problem of
a non-spherical adsorbate mentioned with the use of the
spherical potential in the previous example.

The Kihara core model employing a Lennard-Jones type
(m-n) potential is known to be of value when studying non-
spherical gaseous mixtures. It is a relatively easy equation
to work with and contains only two parameters, ρ_o and $\frac{u_o}{k}$.
Due to its ease of use and value in working with non-spherical
molecules, an attempt is in order to extend it in its original
form to gas-solid interaction studies.

CHAPTER II

THE KIHARA CORE MODEL THEORY

In the study of non-spherical gas molecules Taro Kihara[8,9] developed a theory based upon a concept which he termed the core of the molecule. This theory allows the Lennard-Jones model of molecules with spherical symmetry to be adapted to non-spherical molecules without sacrificing the integrability of the second virial coefficient. The essential generalization exists in the definition of the intermolecular distance, ρ, the intermolecular potential, u, being assumed to be a function of ρ only, u = u(ρ), for which u(o) = ∞. ρ is defined as the shortest distance between cores.

The Core of a Molecule

A description of the core begins with the idea of a convex body, a body in which any line segment whose end points are inside lies entirely in that body. Let C be the convex body of discussion. A second convex body formed by all points whose distances from C are smaller than or equal to 1/2 ρ is called the parallel body of C in the distance of 1/2 ρ. C is then defined as the core of the two parallel bodies.

Consider the core as a convex polyhedron. With N being the number of edges of the polyhedron, the length of

each edge is given by ℓ_1, ℓ_2, ℓ_3,..., ℓ_N and the angle of the ith edge by α_i (i = 1, 2, 3,..., N).

A parallel body of this polyhedron in the distance 1/2 ρ is composed of several parts of a sphere of diameter ρ, several parts of a cylinder of diameter ρ, and several parts of a plane. The surface integral of the mean curvature, M, of this parallel body is therefore given by

$$M = \frac{2}{\rho} \times \text{(surface area of all spherical parts)}$$
$$+ \frac{1}{\rho} \times \text{(surface area of all cylindrical}$$
$$\text{parts)}. \tag{21}$$

Gathering together all the spherical parts gives

$$M = \frac{2}{\rho} \times \text{(surface area of a sphere of diameter } \rho)$$
$$+ \frac{1}{\rho} \times \sum_{i=1}^{N} (\pi - \alpha_i)\frac{\rho}{2} \ell_i. \tag{22}$$

With the introduction of the surface integral of the mean curvature for the core, M_0, equation (22) becomes

$$M = 2\pi\rho + M_0 \tag{23}$$

where

$$M_0 = \frac{1}{2} \sum_{i=1}^{N} (\pi - \alpha_i) \ell_i.$$

By similar reasoning the surface area, S, and the volume, V, of the parallel body are given by the equations

$$S = \pi\rho^2 + M_o\rho + S_o \tag{24}$$

$$V = \frac{\pi}{6}\rho^3 + \frac{1}{4}M_o\rho^2 + \frac{1}{2}S_o\rho + V_o \tag{25}$$

where

S_o = the surface area of the core

V_o = the volume of the core.

Since any convex body can be represented as a limit of polyhedrons, the preceding equations apply to parallel bodies of any convex core.

With the necessary information of interatomic distances and bond angles, an appropriate convex core is depicted within each molecule. Kihara used geometry to prepare Table 1. Using this table and previously mentioned necessary information he was able to prepare Table 2, which is a list of core values for some of the more well-studied non-spherical gas molecules. Figure 3 is an illustration of the core size and shape for the molecules benzene and carbon dioxide.

Derivation of the Kihara Core Model Equation
for Non-Spherical Molecules

For spherically symmetric like molecules the second virial coefficient B can be written in the form
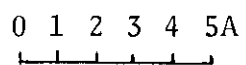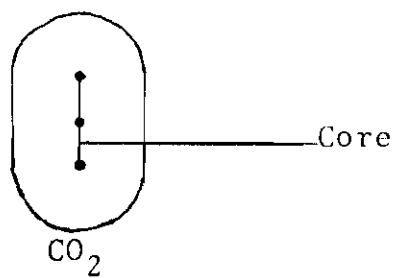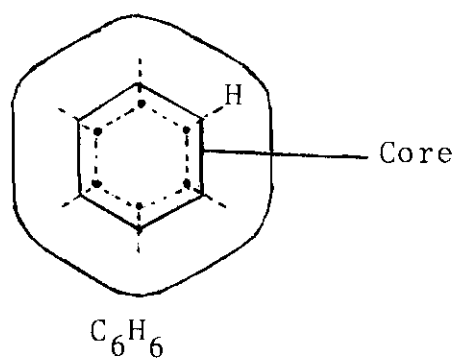
Figure 3. Size and Shape of the Molecular Core for
the Molecules Benzene and Carbon Dioxide

Table 1. Volume, Surface Area, and Surface Integral of the Mean Curvature of Convex Cores

Core	V_o	S_o	M_o
Sphere (radius r)	$\frac{4}{3}\pi r^3$	$4\pi r^2$	$4\pi r$
Rectangular Parallelopiped (length of each edge ℓ_1, ℓ_2, ℓ_3)	$\ell_1 \ell_2 \ell_3$	$2(\ell_1 \ell_2 + \ell_1 \ell_3 + \ell_2 \ell_3)$	$\pi(\ell_1 + \ell_2 + \ell_3)$
Regular Tetrahedron (length of one edge ℓ)	$\dfrac{\ell^3}{6\sqrt{2}}$	$\dfrac{\ell^2}{\sqrt{3}}$	$\dfrac{6\ell}{\tan\sqrt{2}}$
Regular Octahedron (length of one edge ℓ)	$\dfrac{\sqrt{2}\ell^3}{3}$	$\dfrac{2\ell^2}{\sqrt{3}}$	$\dfrac{12\ell}{\cot\sqrt{2}}$
Circular cylinder (length ℓ, radius r)	$\pi r^2 \ell$	$2\pi r(r+\ell)$	$\pi(\pi r + \ell)$
Circular Disk (radius r)	0	$2\pi r^2$	$\pi^2 r$
Rectangle (length of each side ℓ_1, ℓ_2)	0	$2\ell_1 \ell_2$	$\pi(\ell_1 + \ell_2)$
Regular Triangle (length of one side ℓ)	0	$\dfrac{\sqrt{3}\,\ell^2}{2}$	$\dfrac{3}{2}\pi\ell$

Table 1 (concluded)

Core	V_o	S_o	M_o
Regular Hexagon (length of one side ℓ)	0	$\sqrt{3}\ 3\ \ell^2$	$3\pi\ell$
Thin Rod (length ℓ)	0	0	$\pi\ell$

Table 2.   Core Values for Some Well-Characterized Gases

Hydrogen:

$V_o = 0$ $S_o = 0$ $M_o = 2.32 \ \mathring{A}$

Nitrogen:

$V_o = 0$ $S_o = 0$ $M_o = 3.44 \ \mathring{A}$

Carbon Dioxide:

$V_o = 0$ $S_o = 0$ $M_o = 7.23 \ \mathring{A}$

Methane:

$V_o = 0.670 \ \mathring{A}$ $S_o = 5.52 \ \mathring{A}^2$ $M_o = 10.23 \ \mathring{A}$

Carbon Tetrafluoride:

$V_o = 1.47 \ \mathring{A}^3$ $S_o = 9.32 \ \mathring{A}^2$ $M_o = 13.30 \ \mathring{A}$

Ethylene:

$V_o = 0$ $S_o = 3.47 \ \mathring{A}^2$ $M_o = 8.92 \ \mathring{A}$

Benzene:

$V_o = 0$ $S_o = 19.4 \ \mathring{A}^2$ $M_o = 18.2 \ \mathring{A}$

$$B = \int_{r=o}^{r=\infty} [1-e^{-\frac{u(r)}{kT}}]d\ b_o(r) \qquad (26)$$

where

$b_o(r)$ = the second virial coefficient for a rigid

sphere of diameter r, or

$$b_o(r) = \frac{2}{3} \pi r^3.$$

Kihara's core model for non-spherical molecules gives a similar

equation,

$$B = \int_{\rho=o}^{\rho=\infty} [1-e^{-\frac{u(\rho)}{kT}}]d\ b(\rho) + b(o) \qquad (27)$$

where

$b(\rho)$ = the second virial coefficient for the rigid

parallel body of the molecular core in the

distance $1/2\rho$.

By the use of statistical mechanics he was able to show that

$$b(\rho) = V + \frac{1}{4\pi} MS. \qquad (28)$$

Kihara[21] used a Lennard-Jones (m-n) function for $u(\rho)$

(Figure 4),

$$u(\rho) = u_o[\frac{m}{n-m}(\frac{\rho_o}{\rho})^n - \frac{n}{n-m}(\frac{\rho_o}{\rho})^m]\ n>m>3 \qquad (29)$$

where
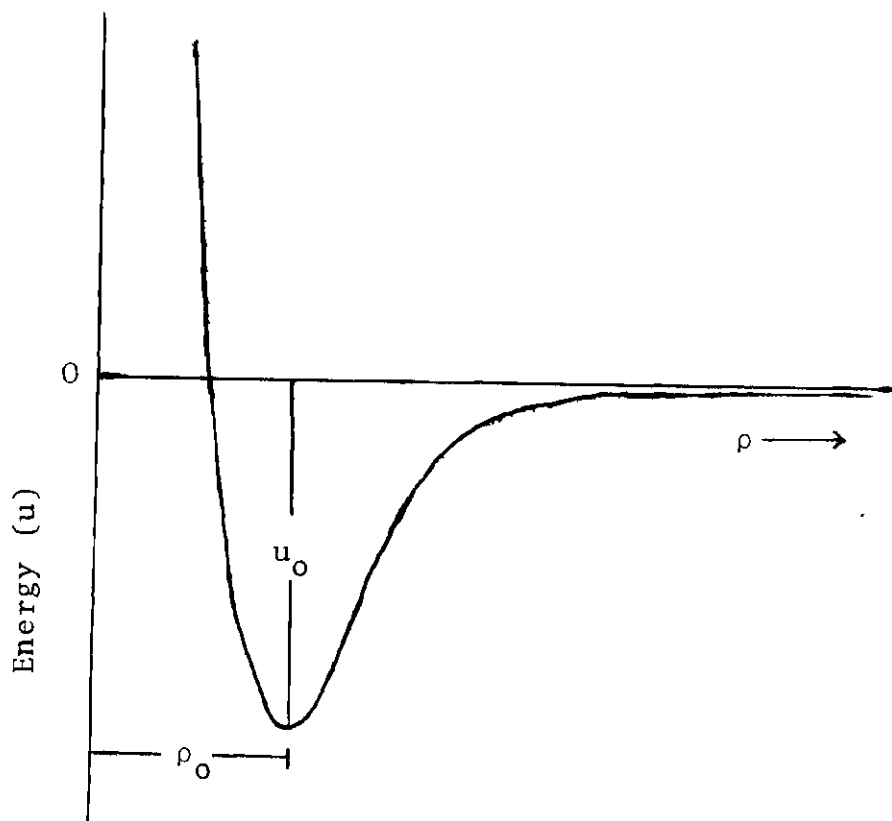
Figure 4.   (m-n) Potential Function Parameters u_o
and ρ_o Used in Kihara's Core Model
Treatment of Non-Spherical Molecules

u_o = the absolute value of the potential minimum

ρ_o = the core separation at the potential minimum

m = the index of attraction

n = the index of repulsion.

Kihara integrated equation (27) using the Lennard-Jones (m-n) potential function for $u(\rho)$ and substituting the equations for V, S, M and $b(\rho)$ (equations (25), (24), (23) and (28), respectively) where necessary. The resulting equation,

$$B = \frac{2}{3} \pi \rho_o^3 F_3(z) + M_o \rho_o^2 F_2(z) \tag{30}$$

$$+ (S_o + \frac{1}{4\pi} M_o^2) \rho_o F_1(z)$$

$$+ (V_o + \frac{1}{4\pi} M_o S_o)$$

where

$$F_s(z) = -\frac{s}{n} \sum_{t=o}^{\infty} \frac{1}{t!} \Gamma(\frac{tm-s}{n}) (\frac{n}{m})^t (z\frac{m}{n-m})^{[(n-m)t+s]/n}$$

$$z = \frac{u_o}{kT}$$

$$s = 1, 2, \text{ or } 3,$$

is Kihara's core model equation for the second virial coefficient of like, non-spherical molecules.

The equation for unlike molecules is derived in the remainder of this chapter. It is similar to that for like molecules and is accomplished by the use of statistical mechanics and relationships developed by Isihara[10,11] and

Minkowski[12].

When the equation for like molecules (equation 27) is extended to unlike molecules, A and B, the second virial coefficient is given by

$$B_{AB} = \int_{\rho=o}^{\rho=\infty} [1-e^{\frac{u_{AB}(\rho)}{kT}}] db_{AB}(\rho) + b_{AB}(o) \qquad (31)$$

where

$$b_{AB}(\rho) = \frac{V_A + V_B}{2} + \frac{M_B S_A + M_A S_B}{8\pi} \qquad (32)$$

$$M_A = 2\pi\rho + M_{OA} \qquad (33)$$

$$S_A = \pi\rho^2 + M_{OA}\rho + S_{OA} \qquad (34)$$

$$V_A = \frac{\pi}{6}\rho^3 + \frac{1}{4}M_{OA}\rho^2 + \frac{1}{2}S_{OA}\rho + V_{OA} \qquad (35)$$

$$M_B = 2\pi\rho + M_{OB} \qquad (36)$$

$$S_B = \pi\rho^2 + M_{OB}\rho + S_{OB} \qquad (37)$$

$$V_B = \frac{\pi}{6}\rho^3 + \frac{1}{4}M_{OB}\rho^2 + \frac{1}{2}S_{OB}\rho + V_{OB} \qquad (38)$$

and

M_A = the surface integral of the mean curvature of the parallel body of the core of molecule A

M_{OA} = the surface integral of the mean curvature of

the core of molecule A

S_A = the surface area of the parallel body of the core of molecule A

S_{OA} = the surface area of the core of molecule A

V_A = the volume of the parallel body of the core of molecule A

V_{OA} = the volume of the core of molecule A

M_B = the surface integral of the mean curvature of the parallel body of the core of molecule B

M_{OB} = the surface integral of the core of molecule B

S_B = the surface area of the parallel body of the core of molecule B

S_{OB} = the surface area of the core of molecule B

V_B = the volume of the parallel body of the core of molecule B

V_{OB} = the volume of the core of molecule B.

Substituting equations (32), (33), (34), (35), (36), (37), and (38), the Lennard-Jones (m-n) potential function $u_{AB}(\rho)$, and the value for $b_{AB}(\rho)$ where $\rho = o$ into equation (31) gives

$$B_{AB} = \int_{\rho=o}^{\rho=\infty} [1 - \exp\{\frac{-U_{OAB}[(\frac{m}{n-m})(\frac{\rho_{OAB}}{\rho})^n - (\frac{n}{n-m})(\frac{\rho_{OAB}}{\rho})^m]}{kT}\}] \qquad (39)$$

$$[2\pi\rho^2 + (M_{OA} + M_{OB})\rho + \frac{S_{OA} + S_{OB}}{2} + \frac{M_{OA}M_{OB}}{4\pi}]d\rho$$

$$+ \frac{V_{OA} + V_{OB}}{2} + \frac{M_{OB}S_{OA} + M_{OA}S_{OB}}{8\pi} \quad .$$

After multiplying and collecting terms equation (39) can be separated into three integral terms and a constant term,

$$B_{AB} = \int_{\rho=o}^{\rho=\infty} 2\pi [1-\exp\{\frac{-U_{OAB}[(\frac{m}{n-m})(\frac{\rho_{OAB}}{\rho})^n - (\frac{n}{n-m})(\frac{\rho_{OAB}}{\rho})^m]}{kT}\}]\rho^2 d\rho \quad (40a)$$

$$+ \int_{\rho=o}^{\rho=\infty} (M_{OA}+M_{OB})[1-\exp\{\frac{-U_{OAB}[(\frac{m}{n-m})(\frac{\rho_{OAB}}{\rho})^n - (\frac{n}{n-m})(\frac{\rho_{OAB}}{\rho})^m]}{kT}\}]\rho d\rho$$

$$(40b)$$

$$+ \int_{\rho=o}^{\rho=\infty} (\frac{S_{OA}+S_{OB}}{2}+\frac{M_{OA}M_{OB}}{4\pi})[1-\exp\{\frac{-U_{OAB}[(\frac{m}{n-m})(\frac{\rho_{OAB}}{\rho})^n - (\frac{n}{n-m})(\frac{\rho_{OAB}}{\rho})^m]}{kT}\}]d\rho$$

$$(40c)$$

$$+ \frac{V_{OA}+V_{OB}}{2} + \frac{M_{OB}S_{OA}+M_{OA}S_{OB}}{8\pi} . \quad (40d)$$

The values of the integrals can be solved for separately and substituted back into the equation for B_{AB}. Integral (40a) can be written

$$2\pi\int_{\rho=o}^{\rho=\infty} (1-e^{-\frac{a}{\rho^n}} e^{\frac{b}{\rho^m}})\rho^2 d\rho \quad (41)$$

where

$$a = \frac{U_{OAB}}{kT}(\frac{m}{n-m})\rho_{OAB}^n$$

$$b = \frac{U_{OAB}}{kT}(\frac{n}{n-m}) \rho_{OAB}^{m}.$$

Using the expansion

$$e^{X} = 1 + X + \frac{X^2}{2!} + \frac{X^3}{3!} + \ldots,$$

integral (41) becomes

$$2\pi\int_{\rho=0}^{\rho=\infty}[1-e^{-\frac{a}{\rho^n}}(1 + \frac{b}{\rho^m} + \frac{b^2}{2!\rho^{2m}} + \frac{b^3}{3!\rho^{3m}} + \ldots)]\rho^2 d\rho. \qquad (42)$$

After multiplication and a substitution integral (42) becomes

$$-\frac{2\pi a^{\frac{1}{n}}}{n}\int_{o}^{\infty}[1-e^{-x}-e^{-x}(ba^{-\frac{m}{n}}x^{\frac{m}{n}} +\frac{b^2}{2!}a^{-\frac{2m}{n}}x^{\frac{2m}{n}} + \frac{b^3}{3!}a^{-\frac{3m}{n}}x^{\frac{3m}{n}} + \ldots)] \qquad (43)$$

$$(a^{\frac{2}{n}}x^{-\frac{2}{n}})(x^{-(\frac{n+1}{n})})dx$$

where

$$x = \frac{a}{\rho^n}.$$

Collecting terms and dividing integral (43) into two parts gives

$$-\frac{2\pi a^{\frac{3}{n}}}{n}\int_{o}^{\infty}(1-e^{-x}) X^{-(\frac{n+3}{n})} dx \qquad (44a)$$

$$+ \frac{2\pi a^{\frac{3}{n}}}{n} \int_0^\infty e^{-x} (ba^{-\frac{m}{n}} x^{-(\frac{n-m+3}{n})} + \frac{b^2}{2!} a^{-\frac{2m}{n}} x^{-(\frac{n-2m+3}{n})} \qquad (44b)$$

$$+ \frac{b^3}{3!} a^{-\frac{3m}{n}} x^{-(\frac{n-3m+3}{n})} + \dots] dx.$$

The integral (44a) and (44b) are solved separately. Integrating integral (44a) by parts gives

$$-\frac{2\pi a^{\frac{3}{n}}}{n} ([\frac{n}{3} e^{-x} x^{-\frac{3}{n}}]_0^\infty + \frac{n}{3} \int_0^\infty e^{-x} x^{-\frac{3}{n}} dx). \qquad (45)$$

Taking the limits of the expression

$$[\frac{n}{3} e^{-x} x^{-\frac{3}{n}}]_0^\infty$$

it is found to be zero. By the use of the gamma function,

$$\Gamma(n) = \int_0^\infty e^{-x} x^{n-1} dx,$$

the remainder of expression (45) becomes

$$-\frac{2\pi a^{\frac{3}{n}}}{3} \Gamma(\frac{n-3}{n}). \qquad (46)$$

Expression (44b) can also be simplified by use of the gamma function to give

$$\frac{2\pi a^{\frac{3}{n}}}{n}[ba^{-\frac{m}{n}}\Gamma(\frac{m-3}{n}) + \frac{b^2}{2!}a^{-\frac{2m}{n}}\Gamma(\frac{2m-3}{n}) + \frac{b^3}{3!}a^{-\frac{3m}{n}}\Gamma(\frac{3m-3}{n}) + ...] \quad (47)$$

which can be rewritten as

$$\frac{2\pi a^{\frac{3}{n}}}{n}\sum_{\tau=1}^{\infty}\frac{b^\tau}{\tau!}a^{-\frac{\tau m}{n}}\Gamma(\frac{\tau m-3}{n}). \quad (48)$$

The integrals (40b) and (40c) can be solved by the same method and equation (40) can be written as

$$B_{AB} = \frac{2\pi a^{\frac{3}{n}}}{n}\sum_{\tau=1}^{\infty}\frac{b^\tau}{\tau!}a^{-\frac{\tau m}{n}}\Gamma(\frac{\tau m-3}{n}) - \frac{2\pi a^{\frac{3}{n}}}{3}\Gamma(\frac{n-3}{n}) \quad (49)$$

$$+ (M_{OA}+M_{OB})\frac{a^{\frac{2}{n}}}{n}\sum_{\tau=1}^{\infty}\frac{b^\tau}{\tau!}a^{-\frac{\tau m}{n}}\Gamma(\frac{\tau m-2}{n})$$

$$- (M_{OA}+M_{OB})\frac{a^{\frac{2}{n}}}{2}\Gamma(\frac{n-2}{n})$$

$$+ (\frac{S_{OA}+S_{OB}}{2}+\frac{M_{OA}M_{OB}}{4\pi})\frac{a^{\frac{1}{n}}}{n}\sum_{\tau=1}^{\infty}\frac{b^\tau}{\tau!}a^{-\frac{\tau m}{n}}\Gamma(\frac{\tau m-1}{n})$$

$$- (\frac{S_{OA}+S_{OB}}{2}+\frac{M_{OA}M_{OB}}{4\pi})a^{\frac{1}{n}}\Gamma(\frac{n-1}{n})$$

$$+ \frac{V_{OA}+V_{OB}}{2} + \frac{M_{OB}S_{OA}+M_{OA}S_{OB}}{8\pi}.$$

After the substitutions for a and b are made, equation (49)

becomes

$$B_{AB} = 2\pi \left(\frac{U_{OAB}}{kT}\right)^{\frac{3}{n}} \left(\frac{m}{n-m}\right)^{\frac{3}{n}} \rho_{OAB}{}^3 \left[\frac{1}{n} \sum_{\tau=1}^{\infty} \left(\frac{U_{OAB}}{kT}\right)^{\frac{\tau(n-m)}{n}} \left(\frac{n}{n-m}\right)^{\tau} \left(\frac{m}{n-m}\right)^{-\frac{\tau m}{n}} \frac{1}{\tau!}\Gamma\left(\frac{\tau m-3}{n}\right)\right.$$

$$\left. - \frac{1}{3}\,\Gamma\left(\frac{n-3}{n}\right)\right]$$

(50)

$$+ \left(\frac{U_{OAB}}{kT}\right)^{\frac{2}{n}} \left(\frac{m}{n-m}\right)^{\frac{2}{n}} \rho_{OAB}{}^2 (M_{OA}+M_{OB}) \left[\frac{1}{n} \sum_{\tau=1}^{\infty} \left(\frac{U_{OAB}}{kT}\right)^{\frac{\tau(n-m)}{n}}\right.$$

$$\left.\left(\frac{n}{n-m}\right)^{\tau} \left(\frac{m}{n-m}\right)^{\frac{-\tau m}{n}} \frac{1}{\tau!}\,\Gamma\left(\frac{\tau m-2}{n}\right) - \frac{1}{2}\,\Gamma\left(\frac{n-2}{n}\right)\right]$$

$$+ \left(\frac{U_{OAB}}{kT}\right)^{\frac{1}{n}} \left(\frac{m}{n-m}\right)^{\frac{1}{n}} \rho_{OAB} \left(\frac{S_{OA}+S_{OB}}{2}+\frac{M_{OA}M_{OB}}{4\pi}\right) \left[\frac{1}{n} \sum_{\tau=1}^{\infty} \left(\frac{U_{OAB}}{kT}\right)^{\frac{\tau(n-m)}{n}}\right.$$

$$\left.\left(\frac{n}{n-m}\right)^{\tau} \left(\frac{m}{n-m}\right)^{\frac{-\tau m}{n}} \frac{1}{\tau!}\Gamma\left(\frac{\tau m-1}{n}\right) - \Gamma\left(\frac{n-1}{n}\right)\right]$$

$$+ \frac{V_{OA}+V_{OB}}{2} + \frac{M_{OB}S_{OA}+M_{OA}S_{OB}}{8\pi}\,.$$

(50)

The gamma functions enclosed within each set of brackets can be combined, and the terms associated with each set of brackets can be written in such a way that equation (51) now becomes the simplified form for the second virial coefficient of unlike gases using the Kihara core model.

$$B_{AB} = \frac{2}{3} \pi \rho_{OAB}^3 \ F_3(\frac{U_{OAB}}{kT}) + (\frac{M_{OA}+M_{OB}}{2}) \rho_{OAB}^2 \ F_2(\frac{U_{OAB}}{kT}) \qquad (51)$$

$$+ \ (\frac{S_{OA}+S_{OB}}{2}+\frac{M_{OA}M_{OB}}{4\pi}) \rho_{OAB} \ F_1(\frac{U_{OAB}}{kT})$$

$$+ \ (\frac{V_{OA}+V_{OB}}{2})+\frac{M_{OB}S_{OA}+M_{OA}S_{OB}}{8\pi} \qquad (51)$$

where

$$F_s(\frac{U_{OAB}}{kT}) \ = \ -\frac{s}{n} \sum_{t=o}^{\infty} \frac{1}{t!}\Gamma(\frac{tm-s}{n}) (\frac{n}{m})^t [(\frac{m}{n-m}) (\frac{U_{OAB}}{kT})]^{\frac{t(n-m)+s}{n}}$$

$$s \ = \ 1, \ 2, \ 3.$$

CHAPTER III

PROCEDURE AND CALCULATIONS

The Kihara core model equation was applied directly to three well-characterized gas-solid interaction systems. Two of the systems studied employed non-spherical adsorbates, benzene and carbon dioxide, adsorbed onto a graphite surface. The third system consisted of a spherical adsorbate, argon, adsorbed onto graphite. The non-spherical adsorbates were used to see how well the equation applied to non-spherical adsorption studies, while the spherical adsorbate was used to see how well the equation applied to spherical adsorption studies.

The method used for testing the application of the Kihara equation to adsorption studies required the use of some known parameters and experimental B_{2s} values for each system. The two parameters in the Kihara equation are $\frac{U_o}{k}$ and ρ_o. When one of the parameters is known along with corresponding B_{2s} values then the remaining parameter may be best fit to the data. In these test calculations, the $\frac{U_o}{k}$ value was known and ρ_o was adjusted until the B_{2s} calculated using the Kihara equation equaled the experimental value. The calculated ρ_o was then compared with a known z_o or z^* (see Figure 2), depending on which value was found in the

literature. The comparison was used to determine the useful-ness of the equation in physical adsorption studies.

Figure 5 is a comparison of two potential energy curves. The dotted line indicates the potential energy of an adsorbate molecule as a function of the distance between the center of the adsorbate molecule and adsorbent surface. The connected line illustrates the potential energy of the same adsorbate molecule as a function of the distance between the adsorbate core and adsorbent core. The potential minimum has the same value in both cases; therefore, $\frac{U_o}{k}$ has a value equal to $\frac{\varepsilon^*}{k}$. However, due to the basic theory of the two models, the ρ value at the potential minimum, ρ_o, for the core model is a smaller value than the separation distance z^* of the other model. As such, the ρ_o calculated to give a B_{2s} equal to a known B_{2s} for a system with a known $\frac{U_o}{k}$ will be expected to be smaller than z^* for that system.

In Kihara's determinations of B_{2s} for unlike, non-spherical molecules, he used the relationship[9]

$$\rho_{OAB} = \frac{1}{2} \rho_{OAA} + \frac{1}{2} \rho_{OBB} \qquad (52)$$

where ρ_{OAA} = the ρ_o value for like molecules of gas A

ρ_{OBB} = the ρ_o value for like molecules of gas B

to determine a ρ_o value for the unlike molecules A and B. The ρ_o values for the benzene-benzene gas system and the carbon dioxide-carbon dioxide gas system were calculated by
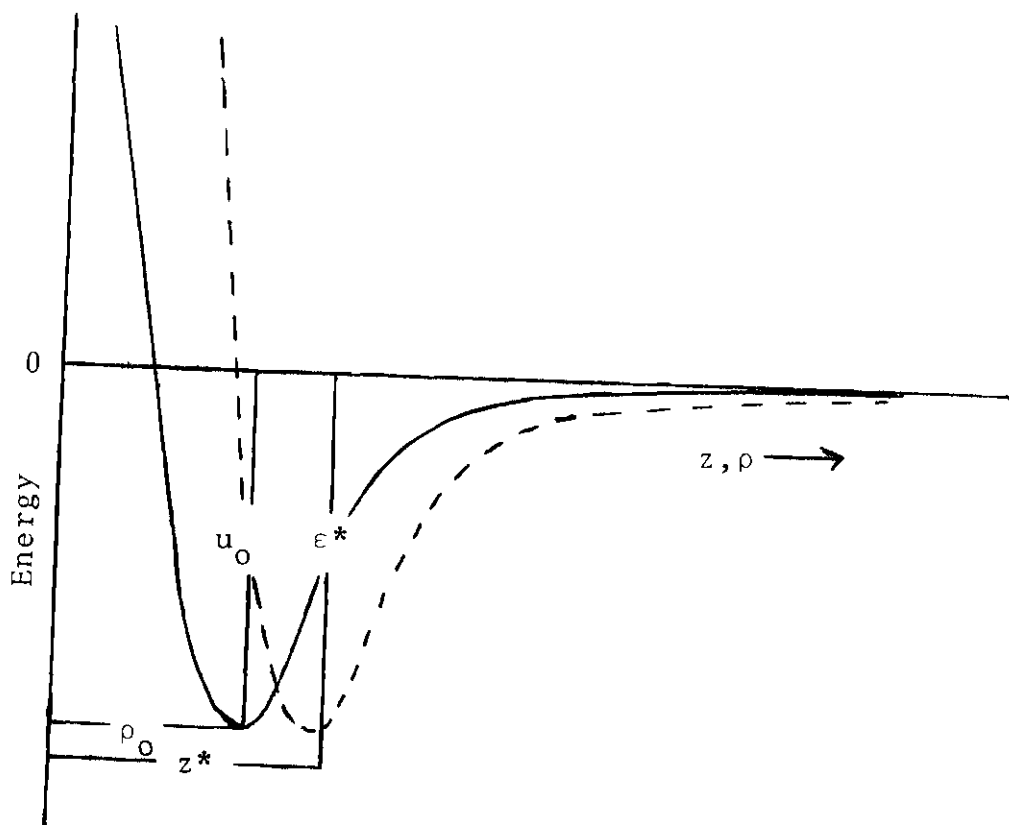
Figure 5. Comparison of the Potential Energy Curves as
a Function of the Distance Between the
Center of the Adsorbate Molecule and the
Adsorbent Surface (- - - -) and as a Function
of the Distance Between Adsorbent Core and
Adsorbate Core (-). The Distance of
Separation is on the Same Scale for Both
ρ and r.

applying equation (52) to the results obtained from the best fit ρ_o method applied to the benzene-graphite and carbon dioxide graphite systems. The result then could be used in other adsorbate-graphite systems desired for study.

The equation used for the calculations was

$$B_{2s} = \frac{2}{3}\ \pi\rho_{OAB}^3 F_3\left(\frac{U_{OAB}}{kT}\right)\ +\ \frac{M_{OA}+M_{OB}}{2})\rho_{OAB}^2 F_2\left(\frac{U_{OAB}}{kT}\right) \tag{53}$$

$$+\ \left(\frac{S_{OA}+S_{OB}}{2}\ +\ \frac{M_{OA}M_{OB}}{4\pi}\right)\rho_{OAB}F_1\left(\frac{U_{OAB}}{kT}\right)$$

$$+\ \frac{V_{OA}+V_{OB}}{2}\ +\ \frac{M_{OB}S_{OA}+M_{OA}S_{OB}}{8\pi}$$

where

$$F_s\left(\frac{U_{OAB}}{kT}\right)\ =\ -\frac{s}{n}\ \sum_{t=0}^{\infty}\ \frac{1}{t!}\Gamma\left(\frac{tm-s}{n}\right)\left(\frac{n}{m}\right)^t\left[\left(\frac{m}{n-m}\right)\left(\frac{U_{OAB}}{kT}\right)\right]^{\frac{t(n-m)+s}{n}}$$

$$s\ =\ 1,\ 2,\ 3$$

B_{2s} = the second gas-solid virial coefficient for gas A and solid B.

The values selected for the Lennard-Jones potential function parameters m and n were 4 and 10, respectively. These values were selected to fill a requirement of the potential $(n>m>3)$, and because earlier adsorption work had not shown a best Lennard-Jones model.

All calculations were accomplished on a Wang 700

programmable calculator. The initial step involved the computation of the $F_s(\frac{U_{OAB}}{kT})$ values by substituting the values for m and n and setting up a program to calculate three values (s = 1, 2, 3) for each $\frac{U_{OAB}}{kT}$. The value of $\frac{U_{OAB}}{kT}$ was started at one and increased by one up through a value of twenty-five. The value of the sum was set so that the limiting t would produce a value less than .001 to be added to the sum. Since the $F_s(\frac{U_{OAB}}{kT})$ values have no core dependency they can be used with any gas-solid interaction system being studied by the Kihara equation and employing the same values for m and n. A list of the $F_s(\frac{U_{OAB}}{kT})$ values is given in Table 3.

The Graphite Core

The three systems selected for study employed graphite adsorbents. Due to the nongaseous nature of the graphite particles it was difficult to determine a core value for the graphite. An approximation was made by assuming the graphite to be small spheres and the core diameter to be slightly smaller than the sphere diameter. Pierotti's adsorption studies[7] have shown the graphite surface area to be approximately 11.7 square meters per gram. Using this value for the surface area, the core values taken from Table 1, and the density of graphite[13], it was possible to calculate a radius for the spherical graphite core:

Table 3. $F_S(\frac{U_o}{kT})$ Values. The Index of Attraction, m, is Equal to 4, and the Index of Repulsion, n, is Equal to 10.

$\frac{U_o}{kT}$	$-F_3(\frac{U_o}{kT})$	$-F_2(\frac{U_o}{kT})$	$-F_1(\frac{U_o}{kT})$
1	5.3033×10^0	1.520×10^0	2.57×10^{-3}
2	1.4113×10^1	5.4321×10^0	1.5640×10^0
3	2.9424×10^1	1.3301×10^1	4.9813×10^0
4	5.9651×10^1	3.0422×10^1	1.2759×10^1
5	1.2535×10^2	6.9874×10^1	3.1181×10^1
6	2.7755×10^2	1.6435×10^2	7.6045×10^1
7	6.4446×10^2	3.9644×10^2	1.8744×10^2
8	1.5516×10^3	9.7665×10^2	4.6789×10^2
9	3.8313×10^3	2.4453×10^3	1.1813×10^3
10	9.6269×10^3	6.1967×10^3	3.0102×10^3
11	2.4484×10^4	1.5847×10^4	7.7283×10^3
12	6.2814×10^4	4.0814×10^4	1.9961×10^4
13	1.6221×10^5	1.0569×10^5	5.1805×10^4
14	4.2101×10^5	2.7492×10^5	1.3500×10^5
15	1.0972×10^6	7.1774×10^5	3.5296×10^5
16	2.8692×10^6	18796×10^6	9.2548×10^5
17	7.5295×10^6	4.936×10^6	2.4327×10^6
18	1.9781×10^7	1.2983×10^7	6.9080×10^6
19	5.2115×10^7	3.4251×10^7	1.6911×10^7
20	13755×10^8	9.0479×10^7	4.4705×10^7
21	3.6367×10^8	2.3939×10^8	1.1835×10^8
22	8.6291×10^8	6.3424×10^8	3.1376×10^8
23	2.5529×10^9	1.6825×10^9	8.3276×10^9
24	6.7765×10^9	4.4685×10^9	2.2127×10^{10}
25	1.8007×10^{10}	1.1880×10^{10}	5.8852×10^{10}

$$\frac{\text{(Surface Area/Particle)}}{\text{(Density)} \times \text{(Volume/Particle)}} = \text{Surface Area/Unit Weight}$$

$$\frac{4\pi r^2}{(2.24 \text{ gm/cm}^3) \times (4/3 \ \pi r^3)} = 11.7 \ m^2/gm$$

$$r = 1.145 \times 10^{-5} \text{ cm.}$$

When the graphite core has the above radius the core values are calculated to be

$$M_o = 1.44 \times 10^{-4} \text{ cm}$$

$$S_o = 1.65 \times 10^{-9} \text{ cm}^2$$

$$V_o = 6.28 \times 10^{-15} \text{ cm}^3.$$

The Benzene Graphite System

The benzene-graphite system was selected for initial calculations. The benzene core values were taken from Kihara's calculations and found to be

$$M_o = 1.82 \times 10^{-7} \text{ cm}$$

$$S_o = 1.94 \times 10^{-15} \text{ cm}^2$$

$$V_o = 0.$$

The known values used for the benzene-graphite system were taken from experimental values listed by Pierotti and

Thomas[7] and are listed below:

$$\frac{\varepsilon^*}{k} = 5510°K \qquad\qquad z^* = 3.43 \times 10^{-8}\ cm$$

Temperature (°K)	$-B_{2s}$ (cm^3/gm)
273	2772
288	1010
293	800
298	488
303	354
308	307
323	152 .

A plot of log B_{2s} vs. $\frac{\varepsilon^*}{kT}$ is not exactly linear in this region; however, it is near enough so that a linear regression of the data can be made. The results are plotted in Figure 6. The linear regression was necessary to determine B_{2s} at whole number values of $\frac{\varepsilon^*}{kT}$.

The next step in the procedure was to use Kihara's equation to calculate a value of ρ_0 to best fit experimental data. The $\frac{U_0}{k}$ value was set equal to the known value of $\frac{\varepsilon^*}{k}$, and the $\frac{U_0}{kT}$ value was selected to lie within the limits of the known $\frac{\varepsilon^*}{kT}$ values. From the linear regression of the known data the B_{2s} value at $\frac{\varepsilon^*}{kT} = 19$ was found to equal -782 cm^3/gm. Using the Kihara equation and substituting the value of $\frac{U_0}{kT} = 19$ and $B_{2s} = -782$ cm^3/gm, ρ_0 was adjusted (to the nearest $.1 \times 10^{-10}$ cm) until B_{2s} was best fit (Figure 7). The ρ_0 value of 7.9×10^{-10} cm was selected as the best fit ρ_0 for the benzene-graphite system. This best fit value of ρ_0 was used to calculate a set of B_{2s} values for the benzene-

$$\text{Log } B_{2s} = (.36166)(\frac{\epsilon*}{kT}) + (-3.9779)$$

$$\frac{\epsilon*}{kT} = 19 \qquad\qquad B_{2s} = -782.66 \text{ cm}^3/\text{gm}$$

$$\frac{\epsilon*}{kT} = 17 \qquad\qquad B_{2s} = -148.00 \text{ cm}^3/\text{gm}$$
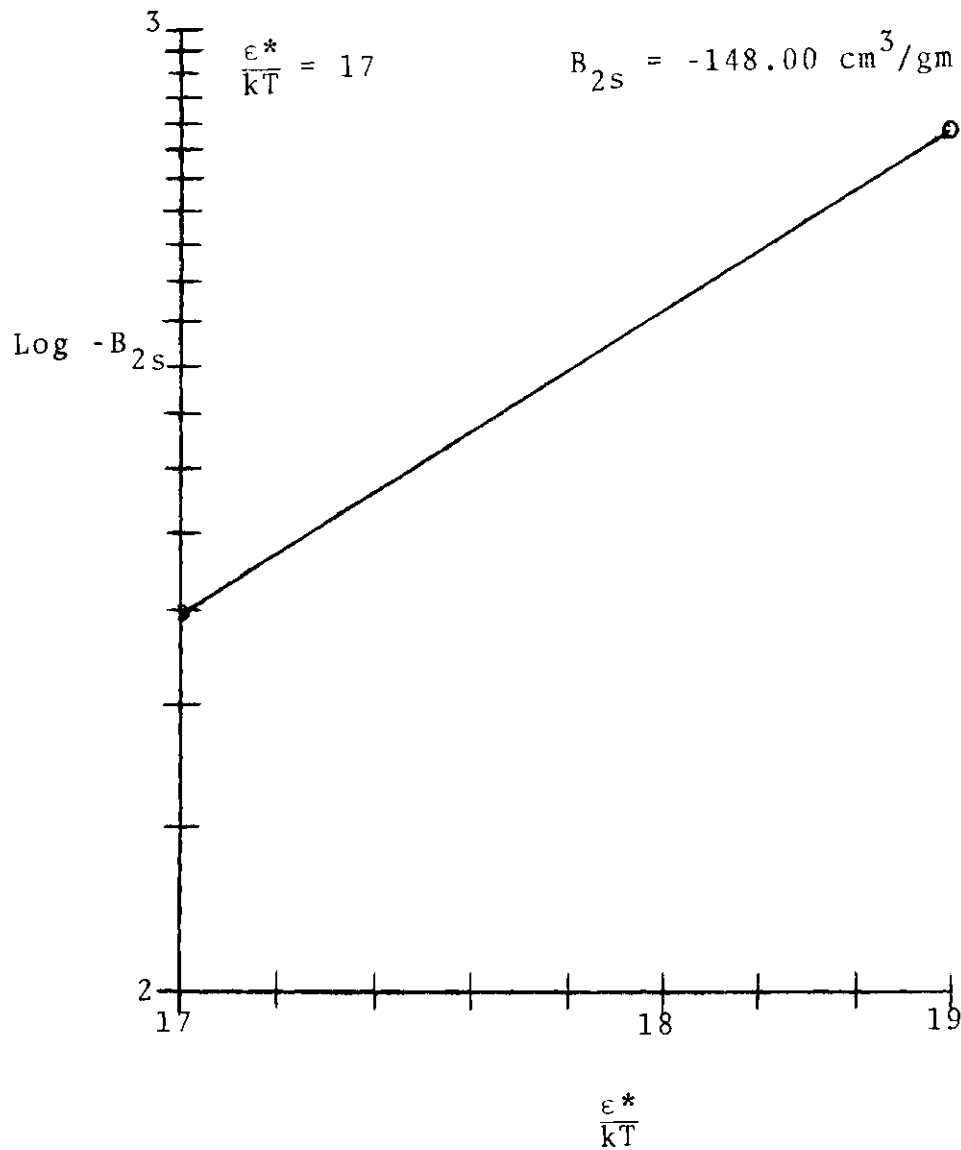
Figure 6. Linear Regression Plot of Benzene-
Graphite Adsorption Data

$$\rho_o = 8 \times 10^{-10} \text{ cm} \qquad B_{2s} = -793.346 \text{ cm}^3/\text{gm}$$

$$\rho_o = 7.5 \times 10^{-10} \text{ cm} \qquad B_{2s} = -743.741 \text{ cm}^3/\text{gm}$$

$$\rho_o = 5 \times 10^{-10} \text{ cm} \qquad B_{2s} = -495.731 \text{ cm}^3/\text{gm}$$
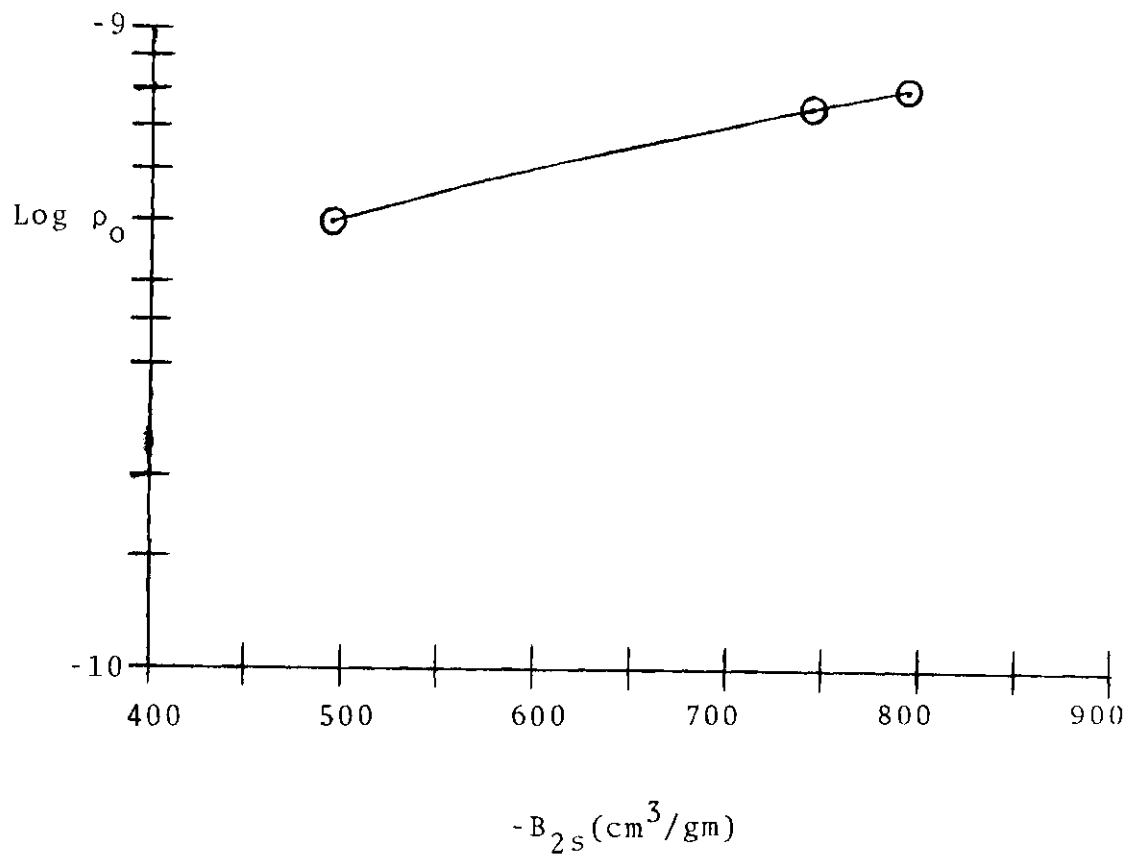

Figure 7.   Best Fit ρ_o for the Benzene-Graphite System

$\dfrac{U_o}{kT} = 19$, $B_{2s} = -782 \text{ cm}^3/\text{gm}$.

graphite system. The results are listed in Table 4.

The Carbon Dioxide-Graphite Systems

The second series of calculations were performed on the carbon dioxide-graphite system. The carbon dioxide core values were taken from Table 2 and found to be

$$M_o = 7.23 \times 10^{-8} \text{ cm}$$

$$S_o = 0$$

$$V_o = 0.$$

The graphite core values were calculated earlier in this chapter. The known values were taken from work done by Myers and Prausnitz[14] and were found to be

$$\frac{\varepsilon^*}{k} = 1670°K \qquad Z_o = 2.13 \times 10^{-8} \text{ cm}$$

Temperature (°K)	B_{2s} (cm^3/gm)
273.15	-.2448
300.07	-.1501
300.64	-.1470
307.67	-.1342
309.22	-.1270 .

A plot of log B_{2s} vs. $\frac{\varepsilon^*}{kT}$ taken from values obtained by a linear regression of Myers and Prausnitz data is presented in Figure 8. The Kihara equation was then used to calculate the best ρ_o (to the nearest .1 $\times$ 10^{-8} cm) that would give

Table 4. The Second Gas-Solid Virial Coefficients for the Benzene-Graphite System Calculated by Use of the Kihara Equation

$\rho_o = 7.9 \times 10^{-10}$ cm

$\dfrac{U_o}{k} = 5510\,°K$

$\dfrac{U_o}{kT}$	$-B_{2s}(\dfrac{cm^3}{gm})$	$\dfrac{U_o}{kT}$	$-B_{2s}(\dfrac{cm^3}{gm})$
1	-0.22406	14	6.0314
2	-0.22399	15	16.131
3	-0.22383	16	42.611
4	-0.22350	17	112.50
5	-0.22262	18	296.71
6	-0.22054	19	783.93
7	-0.21540	20	2,071.4
8	-0.20238	21	5,484.2
9	-0.16932	22	14,539.
10	-0.08457	23	38,589.
11	0.13410	24	102,530.
12	0.70090	25	272,710.
13	2.1765		

$$\text{Log } B_{2s} = .39115 \left(\frac{\varepsilon^*}{kT}\right) - 3.00252$$

$$\frac{\varepsilon^*}{kT} = 6 \qquad B_{2s} = - .225 \text{ cm}^3/\text{gm}$$

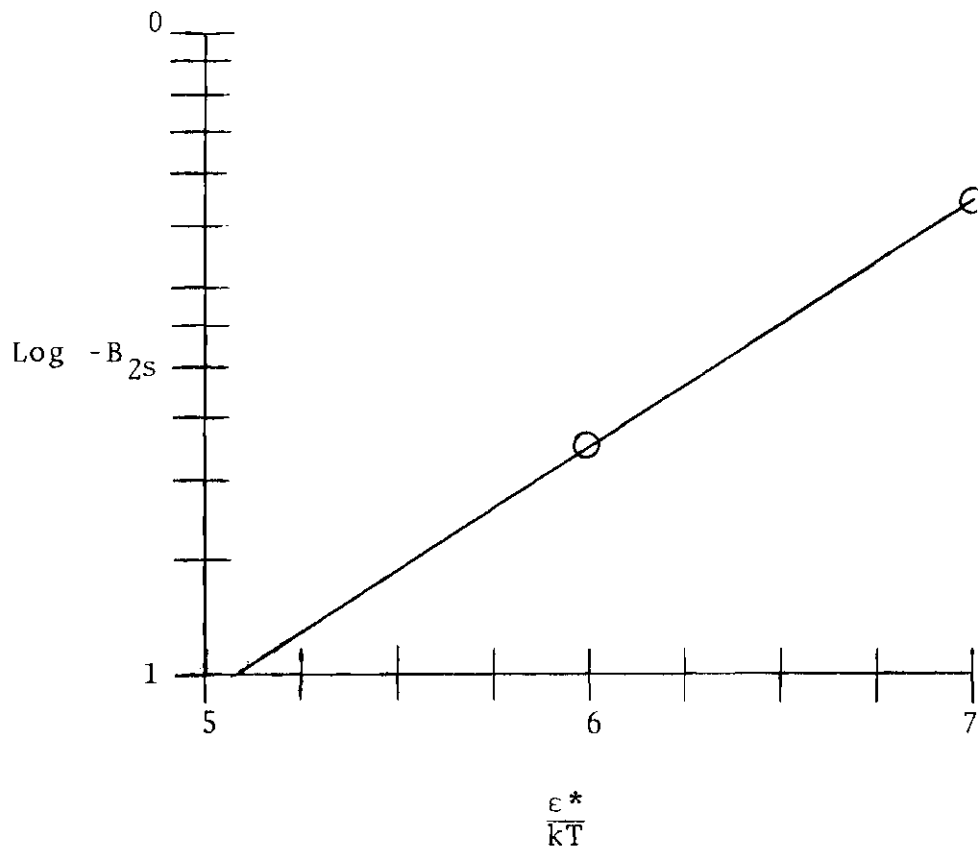$$\frac{\varepsilon^*}{kT} = 7 \qquad B_{2s} = - .545 \text{ cm}^3/\text{gm}$$

Figure 8. Linear Regression of Myers and Prausnitz' Carbon Dioxide-Graphite Adsorption Data

a value of B_{2s} equal to $-.222$ gm/cm^3 when $\frac{U_o}{kT}$ was equal to
6 (see Figure 9). The best ρ_o calculated using this method
was found to equal 9.8×10^{-10} cm. This ρ_o value along with
the core values for carbon dioxide and graphite were substi-
tuted into the Kihara equation to obtain a set of B_{2s} values
for that system (Table 5).

The Argon-Graphite System

The argon-graphite system was next studied to determine
how well the core model theory would apply to spherical
adsorption. The procedure followed was the same as that for
the two non-spherical systems. The core values for argon
were not present in the literature. Therefore, a core was
established in a manner similar to that used to determine a
graphite core. Using the radius of the argon molecule[13] and
the relationships presented in Table 1, the core values
were calculated to be

$$M_o = 1.847 \times 10^{-7} \text{ cm}$$

$$S_o = 2.715 \times 10^{-15} \text{ cm}^2$$

$$V_o = 1.331 \times 10^{-23} \text{ cm}^3.$$

The experimental values for the argon-graphite system
were taken from work done by Sams, Constabaris, and Halsey[15].
The values used were

$$\rho_o = 1.5 \times 10^{-7} \text{ cm} \qquad B_{2s} = -.4635 \text{ cm}^3/\text{gm}$$

$$\rho_o = 1 \times 10^{-7} \text{ cm} \qquad B_{2s} = -.2302 \text{ cm}^3/\text{gm}$$

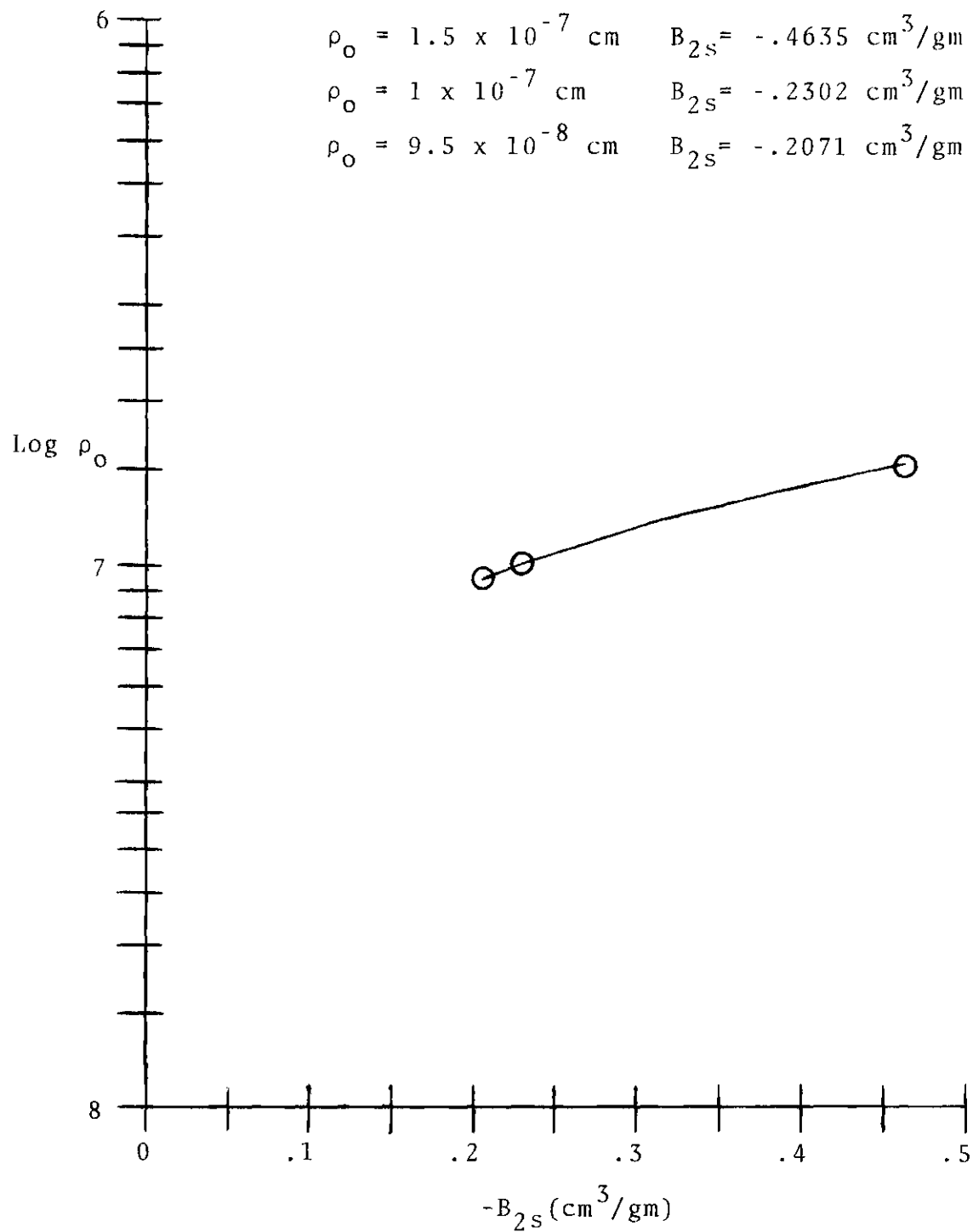$$\rho_o = 9.5 \times 10^{-8} \text{ cm} \qquad B_{2s} = -.2071 \text{ cm}^3/\text{gm}$$

Figure 8. Best Fit ρ_o for the Carbon Dioxide-Graphite System.

$$\frac{U_o}{kT} = 6, \quad B_{2s} = -.222 \text{ cm}^3/\text{gm}.$$

Table 5. The Second Gas-Solid Virial Coefficients for the Carbon Dioxide-Graphite System Calculated by Use of the Kihara Equation

$$\rho_o = 9.8 \times 10^{-8} \text{ cm}$$

$$U_o = 1670°K$$

$\dfrac{U_o}{kT}$	$-B_{2s} \left(\dfrac{cm^3}{gm}\right)$	$\dfrac{U_o}{kT}$	$-B_{2s} \left(\dfrac{cm^3}{gm}\right)$
1	-0.22333	11	44.909
2	-0.21431	12	116.34
3	-0.19431	13	302.29
4	-0.14883	14	788.04
5	-0.04116	15	2,060.7
6	0.22096	16	5,403.6
7	0.87167	17	14,203.
8	2.5097	18	37,414.
9	6.6761	19	98,739.
10	17.357	20	261,020.

$$\frac{\varepsilon^*}{k} = 1071 \qquad\qquad z_o = 2.8 \times 10^{-8} \text{ cm}$$

Temperature (°K)	B_{2s} (cm^3/gm)
140.607	1.4811
145.115	1.1861
150.140	.9422
158.077	.6725
166.135	.4937
175.082	.3655
207.773	.1512
220.393	.1160
240.019	.0813 .

A plot of log B_{2s} vs. $\frac{\varepsilon^*}{kT}$ was made from the values obtained by a linear regression of the experimental data (Figure 10). From this plot a value of $\frac{\varepsilon^*}{kT}$ equal to 6 was selected as the value of $\frac{U_o}{kT}$ to use in the Kihara equation when adjusting ρ_o to find a best value of ρ_o. The B_{2s} value corresponding to the $\frac{\varepsilon^*}{kT}$ value of 6 was found to be -.331 cm^3/gm. The best ρ_o (to the nearest .1 $\times$ 10^{-7} cm) was found to be 1.2 $\times$ 10^{-7} cm. This value of ρ_o was used in the Kihara equation to calculate a set of second gas-solid virial coefficients for the argon-graphite system (Table 6).

The equation used by Kihara to determine ρ_o for the unlike, non-spherical molecules A and B (equation 52) was applied to the benzene-graphite and carbon dioxide-graphite systems to try and determine a $\frac{1}{2}\rho_o$ for the theoretical graphite-graphite system. For the benzene-graphite system,

$$\rho_o(\text{benzene-graphite}) = \frac{1}{2}\rho_o(\text{benzene-benzene}) + \frac{1}{2}\rho_o \ (\text{graphite-graphite})$$

$$\text{Log } B_{2s} = .39986 \left(\frac{\epsilon *}{kT}\right) - 2.8793$$

$\dfrac{\epsilon *}{kT} = 5$ $\qquad$ $B_{2s} = -.1318 \text{ cm}^3/\text{gm}$

$\dfrac{\epsilon *}{kT} = 6$ $\qquad$ $B_{2s} = -.3310 \text{ cm}^3/\text{gm}$

$\dfrac{\epsilon *}{kT} = 7$ $\qquad$ $B_{2s} = -.8312 \text{ cm}^3/\text{gm}$
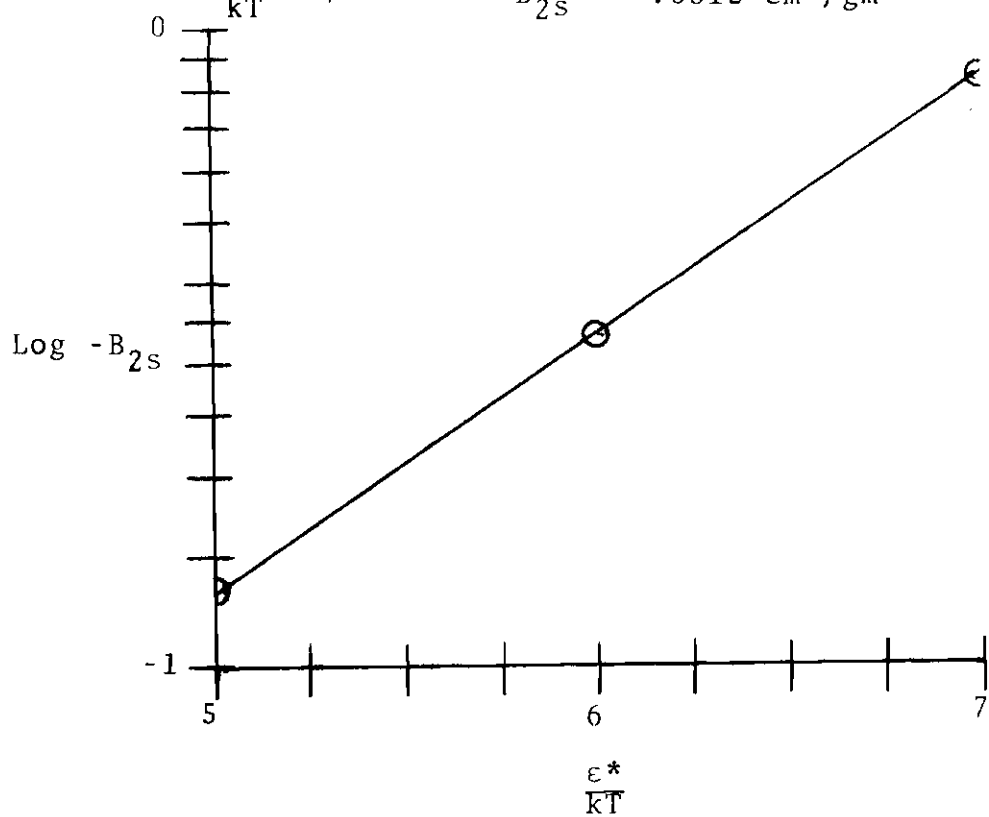

Figure 10. Linear Regression of Sams, Constabaris, and Halsey's Argon-Graphite Adsorption Data

Table 6. The Second Gas-Solid Virial Coefficients for the
Argon-Graphite System Calculated by Use of the
Kihara Equation

$\rho_o = 1.2 \times 10^{-7}$ cm

$\dfrac{U_o}{k} = 1071°K$

$\dfrac{U_o}{kT}$	$-B_{2s}(\dfrac{cm^3}{gm})$	$\dfrac{U_o}{kT}$	$-B_{2s}(\dfrac{cm^3}{gm})$
1	-0.22378	11	55.342
2	-0.21266	12	143.28
3	-0.18803	13	372.21
4	-0.13202	14	970.25
5	0.00056	15	2,537.1
6	0.32331	16	6,652.6
7	1.1245	17	17,487.
8	3.1413	18	46,061.
9	8.2711	19	121,560.
10	21.421	20	321,340.

$\rho_o = 1.5 \times 10^{-7}$ cm $\quad B_{2s} = -.4640$ cm^3/gm

$\rho_o = 1 \times 10^{-7}$ cm $\quad B_{2s} = -.2304$ cm^3/gm

$\rho_o = 9 \times 10^{-8}$ cm $\quad B_{2s} = .1842$ cm^3/gm

$\rho_o = 6 \times 10^{-8}$ cm $\quad B_{2s} = -.0466$ cm^3/gm

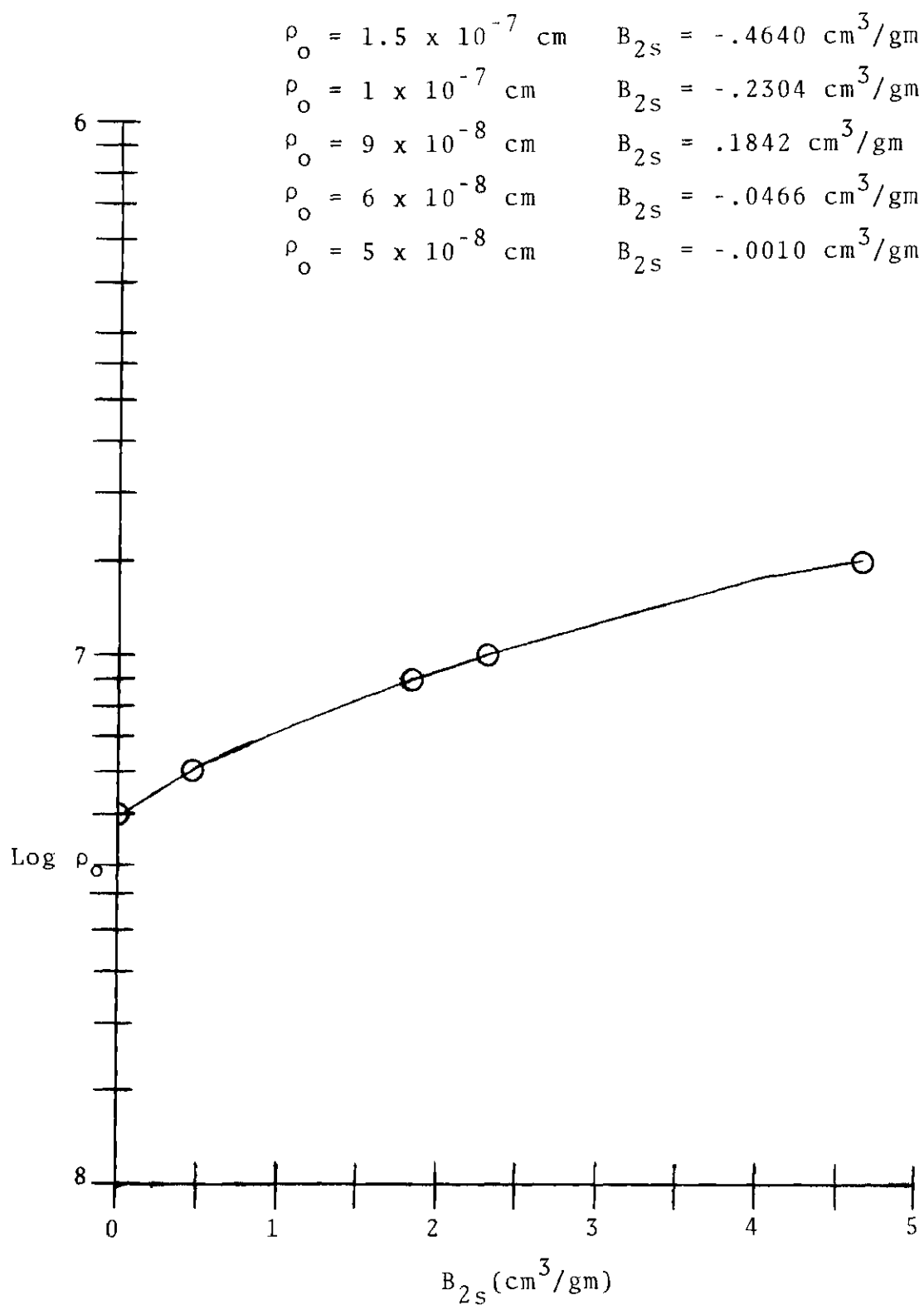$\rho_o = 5 \times 10^{-8}$ cm $\quad B_{2s} = -.0010$ cm^3/gm

Figure 11. Best Fit ρ_o for the Argon-Graphite System. $\frac{U_o}{kT} = 6$, $B_{2s} = -.3233$ cm^3/gm

$$7.9 \times 10^{-10} \text{ cm} = 1.7 \times 10^{-8} \text{ cm} + \frac{1}{2} \rho_o \text{ (graphite-graphite)}$$

$$-1.6 \times 10^{-8} \text{ cm} = \frac{1}{2} \rho_o \text{ (graphite-graphite)}.$$

For the carbon dioxide-graphite system,

$$\rho_o \text{(carbon dioxide-graphite)} = \frac{1}{2} \rho_o \text{(carbon dioxide-carbon dioxide)}$$

$$+ \frac{1}{2} \rho_o \text{ (graphite-graphite)}$$

$$9.8 \times 10^{-8} \text{ cm} = 1.7 \times 10^{-8} \text{ cm} + \frac{1}{2} \rho_o \text{ (graphite-graphite)}$$

$$8.1 \times 10^{-8} \text{ cm} = \frac{1}{2} \rho_o \text{ (graphite-graphite)}.$$

Discussion of Results

The experimental parameters $\frac{\varepsilon^*}{k}$ and z^*, or z_o, are listed opposite the Kihara parameters $\frac{U_o}{k}$ and ρ_o for each gas-solid interaction system studied.

Benzene-Graphite

$$\frac{\varepsilon^*}{k} = 5510°K \qquad\qquad \frac{U_o}{k} = 5510°K$$

$$z^* = 3.43 \times 10^{-8} \text{ cm} \qquad\qquad \rho_o = 7.9 \times 10^{-10} \text{ cm}$$

Carbon Dioxide-Graphite

$$\frac{\varepsilon^*}{k} = 1670°K \qquad\qquad \frac{U_o}{k} = 1670°K$$

$$z_o = 2.13 \times 10^{-8} \text{ cm} \qquad\qquad \rho_o = 9.8 \times 10^{-8} \text{ cm}$$

Argon-Graphite

$$\frac{\varepsilon^*}{k} = 1071°K \qquad\qquad \frac{U_o}{k} = 1071°K$$

$$z_o = 2.8 \times 10^{-8} \text{ cm} \qquad\qquad \rho_o = 1.2 \times 10^{-7} \text{ cm}$$

The Kihara parameter $\frac{U_o}{k}$ was set equal to the known parameter $\frac{\varepsilon^*}{k}$. Using the Kihara equation the ρ_o value was adjusted until a value of B_{2s} corresponding to the experimental value of B_{2s} at a certain temperature was obtained.

In the case of the benzene-graphite system, a comparison of z^* and ρ_o shows z^* to be approximately 40 times greater than ρ_o. A look back at Figure 3 shows the expected ρ_o to be approximately $\frac{1}{2}$ z^* when the benzene molecule is vertical to the graphite surface. The same relationship exists between z^* and ρ_o in the remaining orientations.

A direct comparison between ρ_o and z^* for the carbon dioxide-graphite system was not possible since z^* for the system was not reported in the literature. However, z^* is approximately 1.2 times larger than $z_o{}^7$. An indirect comparison is therefore possible by using the approximate z^* and ρ_o. The results of this comparison show ρ_o to be approximately 4 times larger than z^*. A look at Figure 3 shows the expected ρ_o to be equal to or slightly less than z^* depending on the orientation of the carbon dioxide molecule to the graphite.

A similar situation exists for the argon-graphite system as did for the carbon dioxide-graphite system. The

approximate z^* value is 1.2 times larger than the experimental z_o value. Using this approximate z^*, ρ_o is seen to be approximately 3.5 times larger than z^*. Due to the value given the argon core (with a radius equal to 1.47×10^{-8} cm) the expected ρ_o value was approximately equal to z^* minus the radius of argon, or one-sixth of the calculated value of ρ_o.

An attempt was made to calculate a value of $\frac{1}{2} \rho_o$ for the theoretical graphite-graphite system. The values calculated from the results of the benzene-graphite and carbon dioxide-graphite systems were not in agreement.

CHAPTER IV

CONCLUSIONS AND RECOMMENDATIONS

Conclusions

In the presented study of the non-spherical benzene-
graphite and carbon dioxide-graphite systems and the spherical
argon-graphite system the Kihara core model equation, in its
original form, failed to calculate an acceptable value for
the parameter ρ_0 when a known value was substituted for the
parameter $\dfrac{U_0}{k}$. A consistent value of $\dfrac{1}{2}\rho_0$ for the theoretical
graphite-graphite was not evident from a comparison of the
values obtained from the benzene-graphite system and the
carbon dioxide-graphite system. These results indicate a
failure in the Kihara equation, either in its theoretical
basis or in the calculated core values, to apply to gas-solid
interactions.

Recommendations

Further research in this area should include a study
into the possibility of using a different method to calculate
core values for the graphite adsorbent. Another possibility
exists in the study of other systems employing different
adsorbents.

Whatever future studies are made into this area, the
presented study should serve as a basis from which to begin.

BIBLIOGRAPHY

1. Reginald N. Ramsey, PhD Thesis, Georgia Institute of Technology, 1970.

2. Farrington Daniels and Robert A. Alberty, "Physical Chemistry," John Wiley and Sons, Inc., New York, 1966.

3. J. O. Hirschfelder, C. F. Curtiss, and R. B. Bird, "Molecular Theory of Gases and Liquids," John Wiley and Sons, Inc., New York, 1967.

4. J. J. McAlpin and R. A. Pierotti, Journal of Chemical Physics, 41, 68(1964).

5. J. J. McAlpin and R. A. Pierotti, Journal of Chemical Physics, 42, 1842(1965).

6. T. L. Hill, "Statistical Mechanics," McGraw-Hill Book Company, Inc., New York, 1956.

7. R. A. Pierotti and H. E. Thomas, Physical Adsorption: The Interaction of Gases with Solids, (unpublished manuscript), School of Chemistry, Georgia Institute of Technology, 1970.

8. Taro Kihara, Reviews of Modern Physics, 25, pp. 831-843, 1953.

9. Taro Kihara, Reviews of Modern Physics, 27, pp. 412-423, 1955.

10. A. Isihara, Journal of Chemical Physics, 18, p. 1446, 1950.

11. A. Isihara and F. Hayashidoc, Journal of the Physical Society of Japan, 6, pp. 40 and 46, 1951.

12. H. Minkowski, Mathematische Annalen, 57, p. 447, 1903.

13. "Handbook of Chemistry and Physics," 46th Edition, The Chemical Rubber Co., 1964.

14. A. L. Myers and J. M. Prausnitz, Transactions of the Faraday Society, 61, 1965.

15. J. R. Sams, Jr., G. Constabaus, and G. D. Halsey, Jr., Journal of Physical Chemistry, 64, 1960.